Switching asymmetries in closely coupled magnetic nanostructure arrays

R. E. Dunin-Borkowski[a),b)] and M. R. McCartney
Center for Solid State Science, Arizona State University, Tempe, Arizona 85287-1704

B. Kardynal[b)]
Center for Solid State Electronics Research, Arizona State University, Tempe, Arizona 85287

David J. Smith
Center for Solid State Science, and Department of Physics and Astronomy, Arizona State University, Tempe, Arizona 85287-1504

M. R. Scheinfein
Department of Physics and Astronomy, Arizona State University, Tempe, Arizona 85287-1504

(Received 24 May 1999; accepted for publication 31 August 1999)

Cobalt nanostructures (220 and 300 nm×275 nm×30 nm) were fabricated using electron beam lithography into ordered, close proximity (170 nm) arrays. Domain configurations with accompanying hysteresis loops were measured using off-axis electron holography. Measurements were compared to solutions of the Landau–Lifshitz–Gilbert equations. Both exhibit switching asymmetries due to strong intercell coupling and the presence of a field normal to the cell surface. Magnetic domain configurations during switching depended strongly on the initial conditions, as well as the direction of the perpendicular field relative to the in-plane hysteresis-field direction. © *1999 American Institute of Physics.* [S0003-6951(99)05543-6]

Dynamic memory technology based on magnetic random access memory cells may provide fast, inexpensive, nonvolatile storage over the next decade. Stable, submicron magnetic memory cells, which must have a limited number of magnetically accessible states, are particularly susceptible to the state(s) of their neighbor(s) and to thermal fluctuations. Dense arrays of such cells are prone to intercell coupling.[1–6] Such coupling may scale super-linearly with density since switching in submicron cells often includes propagation of an edge soliton[7] whose stray field is larger than that accompanying vortex-mode[8] switching typical of larger cells. We reported[9] on the domain structure in two rectangular Co cells (275×220×30 and 275×300×30 nm, separated by 170 nm) patterned directly onto self-supporting 55-nm-thick silicon nitride membranes. The magnetic microstructure was characterized using off-axis electron holography[10] in the transmission electron microscope. Hysteresis loops were obtained *in situ* by tilting the specimen in the objective lens field. It will be shown that this out-of-plane field (typically 3600 Oe) breaks the symmetry in the gyromagnetic component of the magnetic moment's motion and imparts a handedness to the switching mode. The present study compares measurements with domain distributions found from the solution of the Landau–Lifshitz–Gilbert (LLG) equations.[11,12] In this letter, we illustrate how switching symmetries can be broken and how the resulting magnetization distributions are altered. Switching asymmetries are seen to originate from the initial magnetization conditions, from interaction between neighboring cells, and from the relative orientation of the perpendicular field relative to the applied in-plane field.

The measured magnetic contribution to the holographic phase for a hysteresis loop[9] is shown in Fig. 1(a). The in-plane field was varied between ±1930 Oe (±30° sample tilt) in an out-of-plane field of 3600 Oe. A color wheel represents the different directions of the in-plane magnetization: pure directions are red (right), yellow (down), green (left), and blue (up). The intensity reflects the magnitude of the in-plane component of the magnetization. Brightest colors have the magnetization lying completely in-plane, with black being completely out-of-plane. The holographic phase contours, which lie almost parallel to the edges of the elements when the applied field is small, follow lines of constant magnetization and their separation is proportional to the integrated in-plane component of the magnetic induction. Local inhomogeneities, magnetization ripple, and reconstruction noise all contribute to the fine detail.

The room temperature simulation parameters for Co include the exchange stiffness, $A=1.55\ \mu$erg/cm and the saturation magnetization, $M_s=1414$ emu/cm^3. The magnetocrystalline anisotropy constant, K, in our polycrystalline films (below 10 nm grain size) was set to zero. Letting $K=0$ is consistent with the observation that the coercivity in our submicron cells (ascribed to shape anisotropy) is much larger than that typical of bulk films of the same thickness, implying that magnetocrystalline anisotropy plays only a minor role in the energetics of switching in ultrasmall cells. The effects of temperature fluctuations were not included. The gyromagnetic frequency, $\gamma=17.6$ MHz/Oe, and damping constant, $\alpha=1$, were used in the LLG equations. Square, in-plane, discrete moments (forming continuous magnetization) ranged in size between 5.39 and 6.875 nm on a side. Changing the out-of-plane discretization between 7.5 and 30 nm produced identical magnetization distributions; hence, a single layer of moments was used here. An all-orders demagnetization field couples all moments in all cells with one another. A hysteresis loop is computed by assigning an initial condition and integrating the LLG equations in a fixed

a)Electronic mail: rafal.db@materials.ox.ac.uk
b)Present address: Department of Materials, Parks Road, Oxford OX1 3PH, UK.

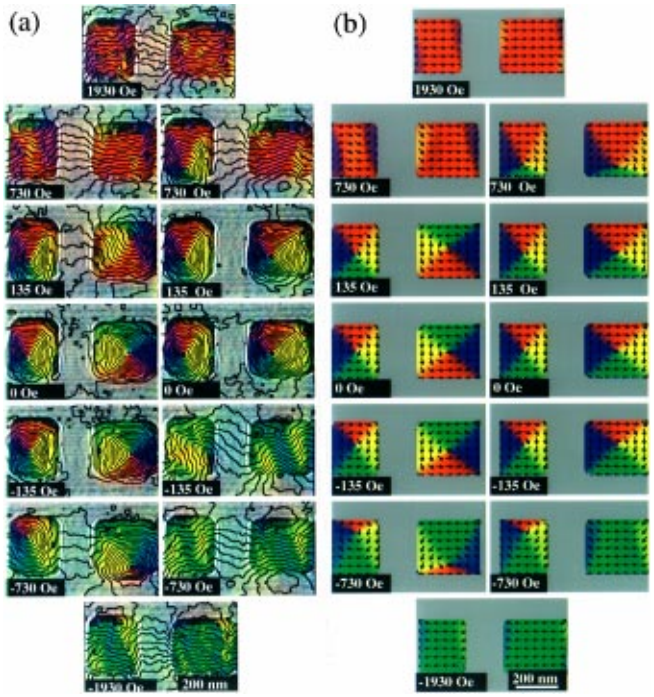

FIG. 1. (a) Magnetic contributions to phases of holograms of 30-nm-thick Co cells during hysteresis loop, obtained with a 200 keV Philips CM200-FEG TEM equipped with Lorentz minilens. Phase contours separated by 0.21π radians. Hysteresis field was applied horizontally when referred to the figure, and should be followed counter-clockwise. Out-of-plane field was 3600 Oe. Colors represent different magnetization directions (see the text) (b) Simulation. Initial states, (small cell) S-State and (large cell) C-State, 3600 Oe field into the page, square corners on cells.

external hysteresis field until equilibrium is reached. The exit criteria (equilibrium) has the largest change in a residual direction cosine of all discretized moments in the grid changing by less than $2-5\times10^{-5}$.

Computed results are shown in Fig. 1(b) where the initial conditions were selected to best match the measurements. The initial state has the small cell (left) oriented in an ''S''-shaped configuration (called A-State in Ref. 7) and the large cell in a modified ''C''-shaped configuration (called B-State in Ref. 7). These states have in-plane magnetization with a small component perpendicular to the in-plane magnetic field in symmetric and antisymmetric configurations respectively. The 3600 Oe vertical field is oriented into the plane. Due to the squareness of its corners, the large bit exhibits a divergence of flux lines on its right edge, coupling the flux back to the smaller bit along both the top and bottom edges of the cell. The simulated vortex helicities match those measured, and almost all of the S-shaped domain structures are reproduced. The main differences are the inability to match the S-shaped domain structure at one end of the reversal cycle, and the fact that vortices form at higher fields in the simulation. The switching asymmetry is illustrated by the simulated hysteresis loops shown in Fig. 2.

Differences in the starting state, often too small to be distinguished visually, are clearly of paramount importance in the formation of subsequent domain structures. Starting states are determined by the magnetic history of each cell, and may differ even though the magnetization may appear to be saturated. For example, further simulations (not shown here) involved making slight changes to the initial conditions

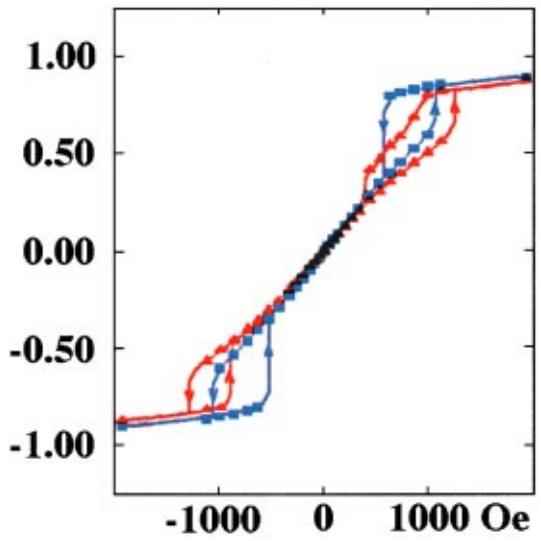

FIG. 2. Hysteresis loops derived from simulations in Fig. 1(b). Red and blue lines represent large and small Co cells, respectively.

and the degree of corner rounding. In one case, the large bit had the magnetization along its right edge pointing upwards, the initial leg of the hysteresis loop (+1930 to −1930 Oe) was (nearly) identical to that shown previously, but the (nearly) saturated state of the large cell at −1930 Oe had a well-defined inverted ''C'' shape. This C-State fixed the handedness of the vortex, which then unrolled with the opposite sense to that in Fig. 1(b) during the second half.

Figure 3 illustrates how neighboring cells alter the magnetic domain structure in the linear array. Three configurations are shown, corresponding to in-plane fields of 432, 333, and 267 Oe during the traversal from 1930 to −1930 Oe. Cells on the left were simulated as a pair, while cells on the right were simulated separately, but displayed as a pair. The domain structure clearly differs as a result of intercell coupling. The energy of the individual cells is higher than that of the pair by 0.68%, 23.4%, and 17.9% for fields of 432, 333, and 267 Oe, respectively. An energy difference of 0.68%

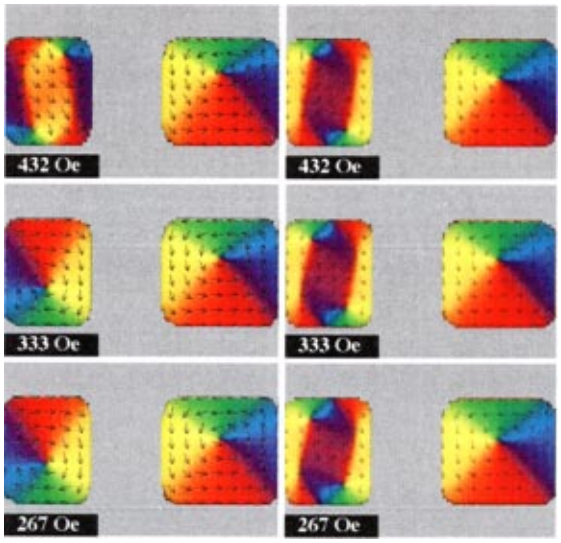

FIG. 3. Simulation. Initial states, (small cell) S-State and (large cell) C-State, 3600 Oe field into the page, rounded corners on bits and applied in-plane fields indicated. Left column simulated for cells together, and right column has each cell simulated separately (shown together).

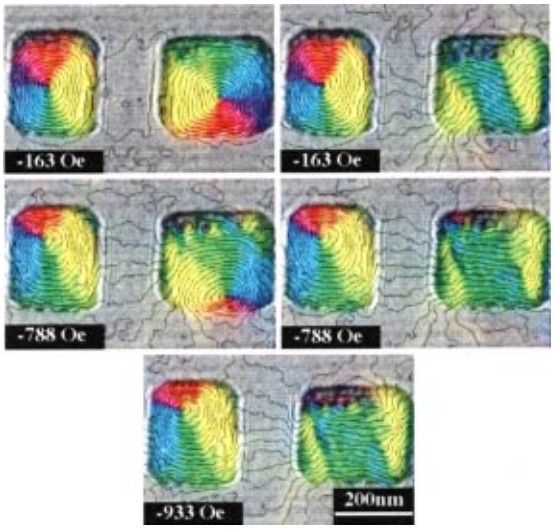

FIG. 4. Measured magnetic contribution to electron holographic phase at one end of magnetization reversal cycle for in-plane fields indicated and out-of-plane field of 3600 Oe. Note incomplete saturation of structure at $H=-990$ Oe.

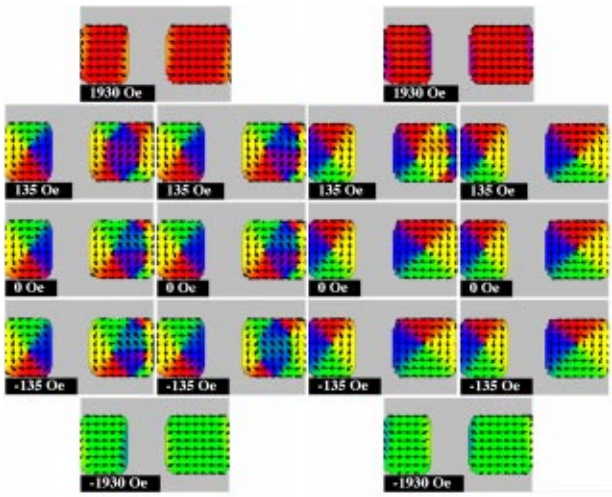

FIG. 5. Simulation: initial states (small cell) S-State and (large cell) S-State, 3600 Oe field into (a) and out of (b) the page, and applied in-plane fields as indicated.

$(1.83\times10^{-11}$ erg) in the apparently similar states (pair versus individual for $H=432$ Oe) reduces the barrier for the small cell between the paired vortex state (resulting from an S-State collapse) and the single, centered vortex state. This energy difference is on the order of the total thermal energy ($E_{\text{th}}=Nk_BT$, $N=V_{\text{cell}}/V_{\text{exchange}}$, and V_{exchange} is a phase correlated region).

The degree to which the magnetization is saturated at the ends of the hysteresis loop has a strong influence on the evolution of the domain structure. Experimental phase images are shown in Fig. 4 for a maximum in-plane field of ±990 Oe. In contrast to Fig. 1(a), the vortex is retained after ''saturation.'' The extent to which vortices[13] persist during switching is of great importance for device applications. The effect can produce variability in switching field that can all but destroy the ability of a magnetic device to discriminate states. That this vortex is stabilized at lower fields in the measurements than in the simulations suggests that the nominal thickness of the films may be greater than 30 nm.

The dependence of the domain structure on the out-of-plane field, often assumed unimportant, is illustrated in Figs. 5(a) and 5(b). Calculations are performed for identical initial conditions (magnetization oriented 10^0 above the horizontal axis) for perpendicular fields (3600 Oe) into and out of the plane, respectively. The perpendicular field defines the handedness of the vortex [CCW in Fig. 5(a) and CW in Fig. 5(b)]. The resulting domain structures illustrate both the effects of the perpendicular field and the proximity of the neighboring cells in trapping the domain states. The collapse of the S-State leads to a vortex pair. This vortex pair must degenerate into a single-centered vortex state by forcing the magnetization to point perpendicular to the cell edge. Intercell coupling blocks the motion of the vortices since the flux closure through the neighboring cell lowers the total energy. Experimentally, complex states such as those illustrated in Figs. 5(a) and 5(b) are often observed.

The sensitivity of magnetization changes to the initial state and the out-of-plane component of the magnetic field emphasizes the need to correlate measurements of magnetic domain structures with micromagnetic simulations. Differences between our experiments and simulations may be ascribed to: variation in cell thickness; including only two cells in the linear array (the end cell was measured); small errors resulting from setting $K=0$; the presence of texture in the Co film; and a small angle between the applied field direction and the line joining the cells. Nevertheless, our results emphasize that intercell coupling must not be overlooked in the design of high density magnetic memory devices.

This work was partly supported by an IBM subcontract on the DARPA Advanced MRAM Project under Contract No. MDA-972-96-C-0014. The authors acknowledge use of the Center for High Resolution Electron Microscopy at ASU.

[1] K. J. Kirk, J. N. Chapman, and C. D. W. Wilkinson, Appl. Phys. Lett. **71**, 539 (1997); K. J. Kirk, J. N. Chapman, and C. D. W. Wilkinson, J. Appl. Phys. **85**, 237 (1999).
[2] S. Gider, J. Shi, D. D. Awschalom, P. F. Hopkins, K. L. Campman, A. C. Gossard, A. D. Kent, and S. von Molnar, Appl. Phys. Lett. **69**, 3269 (1996).
[3] R. D. Gomez, M. C. Shih, R. M. H. New, R. F. W. Pease, and R. L. White, J. Appl. Phys. **80**, 342 (1996).
[4] A. D. Kent, T. M. Shaw, S. von Molnar, and D. D. Awschalom, Science **262**, 1249 (1993).
[5] S. Y. Chou, P. R. Krauss, and L. Kong, J. Appl. Phys. **79**, 6101 (1996).
[6] S. A. Rishton, Y. Lu, R. A. Altman, A. C. Marley, X. P. Bian, C. Jahnes, R. Viswanathan, C. Xiao, W. J. Gallagher, and S. S. P. Parkin, Microelectronic Engineering **35**, 249 (1997).
[7] Y. Zheng and J.-G. Zhu, J. Appl. Phys. **81**, 5470 (1997).
[8] J. Shi, T. Zhu, M. Durlam, E. Chen, S. Tehrani, Y. F. Cheng, and J.-G. Zhu, IEEE Trans. Magn. **34**, 997 (1998).
[9] R. E. Dunin-Borkowski, M. R. McCartney, B. Kardynal, and D. J. Smith, J. Appl. Phys. **84**, 374 (1998).
[10] A. Tonomura, Adv. Phys. **41**, 59 (1992).
[11] M. R. Scheinfein, J. Unguris, J. L. Blue, K. J. Coakley, D. T. Pierce, R. J. Celotta, and P. J. Ryan, Phys. Rev. B **43**, 3395 (1991).
[12] LLG Micromagnetics Simulator is a commercially available Landau–Lifshitz–Gilbert equation solver. For information see www.dancris.com/~llg
[13] J. Shi, S. Tehrani, T. Zhu, Y. F. Zheng, and J.-G. Zhu, Appl. Phys. Lett. **74**, 2525 (1999).